JOURNAL OF Applied Polymer SCIENCE

Effect of Different Types of Organoclays and Compatibilizers on the Properties of Polystyrene-Based Nanocomposites

Canan Esma Yeniova, Ulku Yilmazer
Department of Chemical Engineering, Middle East Technical University,06531 Ankara, Turkey

Correspondence to: U. Yilmazer (E-mail: yilmazer@metu.edu.tr)

ABSTRACT: Polystyrene/organoclay nanocomposites were prepared by melt intercalation in the presence of elastomeric impact modifiers. Three different types of organically modified montmorillonites; Cloisite® 30B, 15A, and 25A, were used as reinforcement, whereas poly [styrene-b-(ethylene-*co*-butylene)-b-styrene] (SEBS-g-MA) and poly(ethylene-b-butyl acrylate-b-glycidyl methacrylate) (E-BA-GMA) elastomeric materials were introduced to act as impact modifier. Owing to its single aliphatic tail on its modifier and absence of hydroxyl groups, Cloisite® 25A displayed the best dispersion in the polystyrene matrix, and mostly delaminated silicate layers were obtained in the presence of SEBS-g-MA. This was attributed to the higher viscosity of SEBS-g-MA compared with both E-BA-GMA and poly(styrene-*co*-vinyloxazolin) (PS). In addition, the compatibility between SEBS-g-MA and PS was found to be better in comparison to the compatibility between E-BA-GMA and PS owing to the soluble part of SEBS-g-MA in PS. The clay particles were observed to be located mostly in the dispersed phase leading to larger elastomeric domains compared with binary PS/elastomer blends. The enlargement of the elastomeric domains resulted in higher impact strength values in the presence of organoclay. Good dispersion of Cloisite® 25A in PS/SEBS-g-MA blends enhanced the tensile properties of this nanocomposite produced. It was observed that the change in the strength and stiffness of the ternary nanocomposites mostly depend on the type of the elastomeric material.
 J. Appl. Polym. Sci. 000: 000–000, 2012

KEYWORDS: nanocomposite; organoclay; polystyrene; compatibilization

Received 29 June 2011; accepted 26 April 2012; published online
DOI: 10.1002/app.37968

INTRODUCTION

In nanocomposites, particles with high aspect ratio are dispersed to achieve remarkable improvements in properties such as; strength, stiffness, thermal stability, and barrier properties.[1,2] Among all the potential nanocomposites,[3–5] those based on organoclay display superior mechanical properties compared with unidirectional fiber reinforced polymers owing to reinforcement from the inorganic layers in two rather than in one dimension.[6]

Layered silicates are clay minerals that are generated by the combination of tetrahedral and octahedral sheets with 2 : 1 stacking order. Silica is the main component of the tetrahedral sheets while octahedral sheet comprises diverse elements.[7] For montmorillonite (MMT), Al based octahedral sheets disappear between the tetrahedrons and approximately 1 nm thick layers are formed.[8]

An excess negative charge called as "cation exchange capacity" is created by isomorphic substitution within the silicate layers.[7] These negative charges are balanced by alkali or alkaline earth cations, and the presence of these cations increases the basal spacing of the clay crystal, but it also makes the clay crystal hydrophilic. This hydrophilic clay is turned into organophilic by imparting alkylammonium or alkylphosphonium ions within the clay layers by replacing the cations.[9] Thus, the modified layered silicates become more compatible with the organic nonpolar polymers because of their lower surface energy.[10]

When the interaction between polymer chains and the clay surface is enough to push apart the layers, a disordered array is formed and a delaminated structure can be observed. Nevertheless, this is not always the case. Instead of exfoliation, the polymer chains may be inserted between the clay layers by expanding the interlayer spacing and leaving the stacking order the same,[11,12] or the clay particles may remain as tactoids and the properties stay in the same range as conventional composites with poor properties.[13]

It is established that polystyrene/poly(styrene-co-vinyloxazolin)/organoclay nanocomposites (PS/OPS/organoclay) generally have an intercalated structure.[14–17] Recently, it was attempted to

enhance the interaction between PS and organoclay surface. For instance, Park et al.[18] obtained exfoliated structures in PS/OPS with the help of bilayer type arrangement of the organic modifier. The study reported by Maryam et al.[19] showed that a well dispersed structure can be achieved by intercalating Na-MMT with a copolymer of styrene and vinyl benzyl trimethyl ammonium chloride before melt compounding. Use of polymeric compatibilizer, which creates loops and tails on the clay surface to interact with the thermoplastic melt, is another method to obtain exfoliated structures. These types of materials are also categorized as impact modifiers due to their elastic structure that enhances the impact strength of the polymer matrix. Tanoue et al.[20] applied different screw rotation speeds during the melt compounding of PS/OPS. Park et al.[21] investigated the effects of amorphous styrenic polymer compatibilizer on the microstructure of syndiotactic PS/organophilic clay nanocomposites prepared by the method of melt mixing.

Effects of the elastomeric materials, poly[styrene-b-(ethylene-*co*-butylene)-b-styrene] (SEBS-g-MA) and poly(ethylene-b-butyl acrylate-b-glycidyl methacrylate) (E-BA-GMA), and three different organically modified Na-MMT's on the morphological, flow, mechanical, and thermal properties of PS were investigated in this work. The analyses that were performed by X-Ray Diffraction (XRD), Transmission Electron Microscopy (TEM), Scanning Electron Microscopy (SEM), differential scanning calorimetry (DSC), tensile, and impact tests.

EXPERIMENTAL

Materials

Lacqrene® 1960N, commercial polystyrene, was obtained from TOTAL Petrochemicals. As compatibilizer, Shell Chemicals product Kraton® FG1924X, SEBS-g-MA, and DuPont product Elvaloy® PTW, ethylene/butyl acrylate/glycidyl methacrylate (E-BA-GMA), were used. Three different organophilic clays; Cloisite® 30B, Cloisite® 15A and Cloisite® 25A, were purchased from Southern Clay Products. Their properties and organic modifier structures can be seen from Table I.

Preparation and Characterization of Nanocomposites

The two stage melt compounding was carried out in a corotating Thermo Prism TSE 16 TC intermeshing twin screw extruder ($L/D = 25$). In the first stage; PS, elastomer and organically treated MMT were simultaneously extruded at a screw speed of 300 rpm. During the extrusion process, the temperature profile was kept at 200°C, and the feed rate was set to 25 g/min to obtain 10 wt % Elastomer/4 wt % organoclay/86 wt % PS composition. In the second run extrusion, the mixture was diluted with pure PS to obtain the final desired composition which contained 5 wt % of compatibilizer–elastomer and 2 wt % of organoclay. For comparison purpose, PS/elastomer blends and PS/organoclay binary nanocomposites were also prepared.

To prepare the test specimens, DSM Xplore micro injection molding was used by keeping the mold temperature and melt temperature at 30 and 200°C, respectively.

Rigaku D/MAX 2200/PC based X-ray diffractometer equipped with Cu Kα radiation was used to analyze the nanocomposites. The diffractometer generates X-rays of 1.54 Å wavelength (λ), at a generator tension of 40 kV and a generator current of 40 mA. The diffraction patterns were collected between diffraction angle 2θ from 1° to 10° at a scanning rate of 1°/min. The samples for XRD were obtained from the molded specimens.

Table I. Typical Characteristics of Organoclays

Organoclay	Organic modifier	2theta (θ°)	d-Spacing (Å)	CEC (mequiv./100 g clay)
Cloisite® 30B	MT2EtOH	4.88	d_1: 18.1	90
Cloisite® 15A	2M2HT	2.8	d_1: 31.5	125
		7.1	d_2: 12.4	
Cloisite® 25A	2MHTL8	4.72	d_1: 18.7	95

MT2EtOH: methyl, tallow, bis-2-hydroxyethyl, quaternary ammonium.
2M2HT: dimethyl, dehydrogenated tallow, quaternary ammonium.
2MHTL8: dimethyl, hydrogenated tallow, 2-ethylhexyl quaternary ammonium.

Phillips CM200 TEM operated at 120 kV was used for taking images of the specimens. Ultrathin sectioning was maintained at 70 nm by cutting the samples with a diamond polymer knife at a temperature of −100°C.

The fracture surface of the ternary nanocomposites and binary blends were etched in *n*-Heptane at room temperature until a small degree of deterioration took place. After the etching process, the surfaces were coated with a thin layer of gold, and the morphology was examined by a low voltage JEOL JSM-6400 SEM.

The glass transition temperature measurements of the samples were carried out under nitrogen atmosphere by using DSC-60 Shimadzu differential scanning calorimeter. They were heated from 30°C to 350°C with a heating rate of 20°C/min. Samples about 3 mg were cut from dry tensile bars and placed in aluminum DSC pans. Changes in T_g values were examined for each composition to observe the effects of clay and elastomer type.

Tensile tests were carried out at a strain rate of 0.1 min^{-1} by using Lloyd LR 30K Universal Testing machine, and Ceast Resil Impactor was used to perform the un-notched Charpy impact tests on samples with dimensions of 80 × 10 × 4 mm^3.

RESULTS AND DISCUSSION

XRD Analysis

The first 2θ peak of the XRD patterns are related to the distance between the silicate layers. According to this relation, the reduction in 2θ value indicates an increase in the basal spacing. In intercalated structures, the spacing increases owing to insertion of polymer chains between the clay layers and the characteristic peak shifts to a lower angle. On the contrary, no peak can be observed in the XRD pattern of exfoliated nanocomposites.[2,7,22]

Packing density, stability of the organic modifier, amount of platelet separation, clay surface—polymer matrix, polymer matrix—impact modifier, and even clay surface—impact modifier interactions are internal effects that influence the dispersion level of the clay particles. Among these effects, clay surface—polymer matrix interaction is quite important due to possible reactions between the functional groups of the alkylammonium

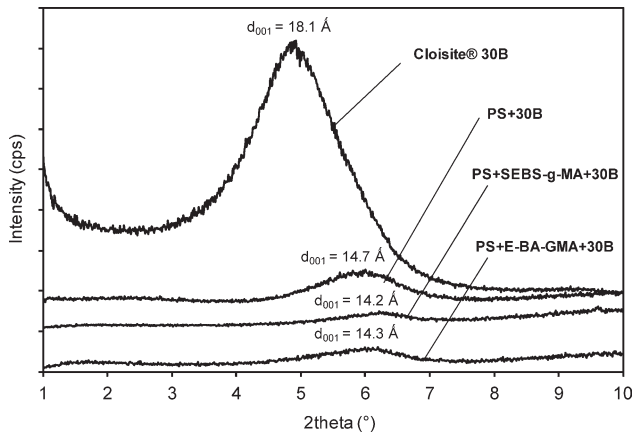

Figure 1. XRD patterns of nanocomposites containing Cloisite® 30B.

cations with the polymer matrix that create a high enforcement on clay platelets and push the platelets apart.[23] Because there is no possibility for the PS matrix to undergo such a reaction with the modifier of the organoclay or the functional groups of compatibilizer, other internal effects become more important. Figure.1 shows the diffraction patterns of pure Cloisite® 30B and nanocomposites prepared with this organoclay. In the binary nanocomposites of PS/Cloisite® 30B, no improvement can be observed in the basal spacing. Due to —OH groups on its organic modifier, Cloisite® 30B has the highest hydrophilic surface among the organoclays used in this study.[24] Thus, its poor dispersion in the highly nonpolar PS matrix is an expected result. In addition, according to Paul et al.[25] the surfactants containing hydroxyl-ethyl units display a high density which is attributed to dense molecular packing in the galleries. This is the result of the hydrogen bonding between the hydroxyl groups of the surfactants and the oxygen of the clay surface which impedes the intercalation of polymer chains into the galleries.

The intercalation of polymer matrix into the galleries of the organoclay was attempted to be achieved by adding an elastomeric compatibilizer phase to the PS/organoclay binary nanocomposites. The elastomeric materials SEBS-g-MA and E-BA-GMA contain functional groups of maleic anhydride and glycidyl methacrylate, respectively. Both functional groups have the ability of reacting with the hydroxyl groups of the clay surface and increasing the adhesion onto polar substances. Thus, it is obvious that, there would be an interaction between the elastomers and modifier of the Cloisite® 30B. However, the ethylene–butylene and butyl-acrylate blocks of the elastomers are incompatible with the layer surface and may repel the clay layer during the intercalation process leading to conventional composites.[21] In addition, Figure 1 shows that the basal spacing of the Cloisite® 30B decreased slightly with both types of elastomers due to decomposition of the organic modifier at extrusion temperature.[20]

The diffraction patterns of nanocomposites containing Cloisite® 15A can be seen from Figure 2. The pure organoclay exhibits two diffraction peaks in its XRD diffractogram. The second peak has a lower intensity than the first peak. In some cases, a secondary peak may result from reflections from the next silicate layer, if its 2θ value is twice that of the first peak.[26,27] However, for Cloisite® 15A reflection from the next silicate layer is not the reason for the presence of the second peak. According to Southern Clay Products, the d-spacing of the unmodified MMT is approximately 12.4 Å, which is the same as the second d-spacing value of Cloisite® 15A, calculated by Bragg's law, as observed in Figure 2. Thus, this second peak corresponds to clay in which the inorganic cations of the smectite clay were not fully replaced by the organic ions.

For the interlayer spacing of the PS/Cloisite® 15A binary nanocomposites no intercalation was observed, whereas the second peak is shifted to the left due to insertion of the PS chains between unmodified clay layers. Cloisite® 15A has the most hydrophobic surface among the organoclays used in this study due lack of polar groups on its modifier, and this absence of functional groups in the organic modifier makes dispersive forces more effective. In addition, its relatively high initial d-spacing makes dispersion of silicate layers easier due to reduced platelet–platelet attraction. Thus, the attraction between nonpolar PS and Cloisite® 15A may be expected to be the highest compared with dispersion of other organoclays used in this study. However, Cloisite® 15A has two long aliphatic tails, and these tails limit the access of polymer chains to the clay surface. Because of these alkyl chains, the interaction between the polymer chains and organoclay platelets cannot overcome the interaction between the organoclay platelets. Thus, alkylammonium compound consisting of one alkyl tail is more effective than the quaternary cation having two alkyl tails in forming exfoliated nanocomposites.[28]

Cloisite® 15A has no possibility to make hydrogen bonding with the functional groups of the elastomeric materials. However, when the ternary nanocomposites are considered, it can be seen that the addition of elastomeric phase slightly increases the d-spacings calculated both from the first peak and the second peak. Besides the internal effects, external effects such as shear intensity applied on the clay platelets is highly related to the level of dispersion, because intercalation and/or exfoliation require diffusion of polymer chains into silicate layers or peel away the top and bottom layers by polymer adsorption and by

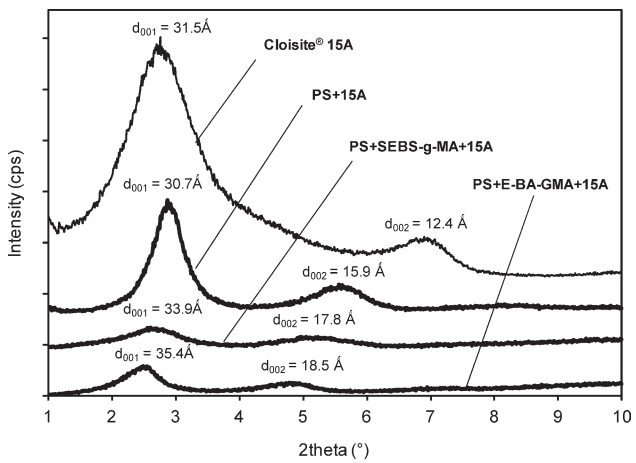

Figure 2. XRD patterns of nanocomposites containing Cloisite® 15A.

Applied Polymer SCIENCE

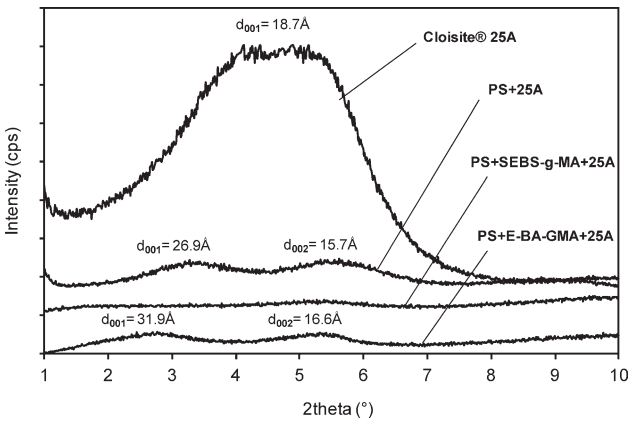

Figure 3. XRD patterns of nanocomposites containing Cloisite® 25A.

the application of shear stress.[29] PS has a lower viscosity than that of the elastomeric material SEBS-g-MA, whereas, it exhibits a greater viscosity than that of E-BA-GMA.[30] Due to increase in viscosity with the addition of SEBS-g-MA, the shear intensity during the extrusion increases, leading to expansion of the d-spacing. In addition, E-BA-GMA containing nanocomposite displayed an intercalated structure and this may be attributed to the high initial d-spacing of Cloisite® 15A. Although the ternary nanocomposite containing E-BA-GMA has a greater basal spacing, the peak intensities for the PS/SEBS-g-MA/Cloisite® 15A nanocomposite are lower indicating good dispersion, due to quite higher viscosity of SEBS-g-MA in comparison to E-BA-GMA.

Among the nanocomposites used in this study, Cloisite® 25A showed the best dispersion. Figure 3 shows the diffraction patterns of binary and ternary Cloisite® 25A containing nanocomposites and the pattern of pure Cloisite® 25A. As can be seen from the pattern of PS/Cloisite® 25A binary nanocomposite, the clay layers remained as tactoids with intercalated polymer chains between the layers and a remarkable improvement occurred in the basal spacing. Although Cloisite® 25A has no secondary

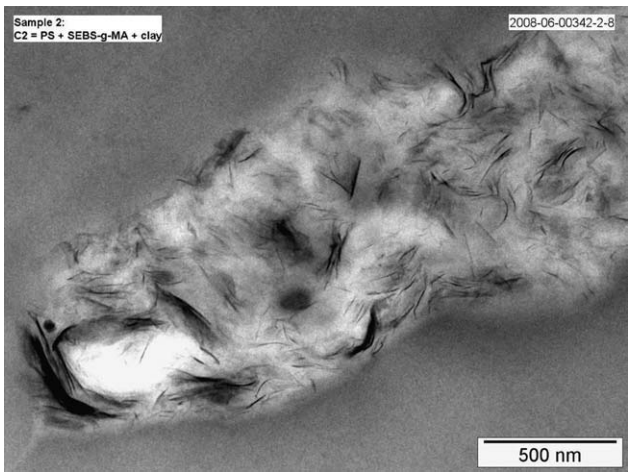

Figure 4. TEM micrograph of PS/SEBS-g-MA/Cloisite® 25A ternary nanocomposite.

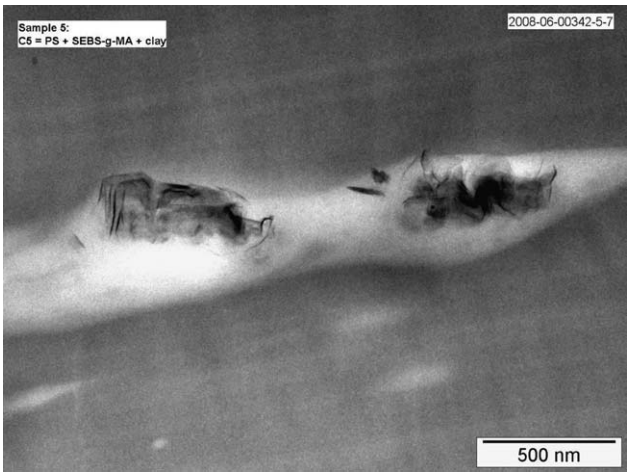

Figure 5. TEM micrograph of PS/SEBS-g-MA/Cloisite® 30B ternary nanocomposite.

peak in its pure powder form a second peak appeared in the binary and ternary nanocomposites. When calculated with Bragg's law, these peaks correspond to a d-spacing value that is approximately twice that of the first characteristic peak. Thus, it can be said that the second peak is due to the reflections from the second silicate layer.

In the ternary nanocomposite containing SEBS-g-MA and Cloisite® 25A, no diffraction peak is observed exhibiting exfoliated structure, whereas for the nanocomposite prepared with E-BA-GMA, a structure in which most of the clay particles are intercalated can be seen. The better dispersion of Cloisite® 25A with SEBS-g-MA can also be partially attributed to its higher viscosity compared with both E-BA-GMA and PS.

TEM Analysis

The features of the local microstructures from TEM give useful detail to the overall picture that is drawn from the XRD results. TEM images of the ternary nanocomposites PS/SEBS-g-MA/Cloisite® 25A and PS/SEBS-g-MA/Cloisite® 30B are displayed in Figures 4 and 5. In these images, the black spots indicate the clay agglomerates. In the micrograph of the nanocomposite containing Cloisite® 25A, the spots appear to be delaminated and have the shape of ribbons indicating a partially intercalated and partially exfoliated structure. However, the XRD result of this nanocomposite displayed full exfoliation as discussed earlier. In this sense, TEM images are more reliable because X-ray beams may hit to a nonuniformly dispersed region of the sample and Bragg's reflection may be eliminated demonstrating exfoliation or it may remain unchanged as in conventional composites owing to low concentration of the organoclay.[15] In accordance with the XRD result of the ternary nanocomposite containing Cloisite® 30B, TEM image reveals a conventional composite structure.

In this study, not only the extent of dispersion of clay layers in nanocomposites was studied, but also the location of the clay particles was detected. In the images, the white regions that encapsulate the clay particles display the elastomeric phase, SEBS-g-MA, and the gray areas show the PS matrix. The reason for

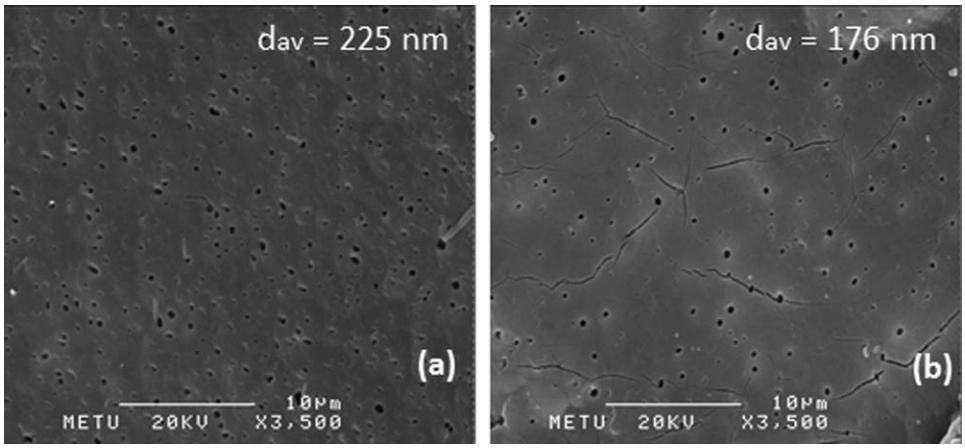

Figure 6. SEM micrographs of (a) PS/SEBS-g-MA and (b) PS/E-BA-GMA binary blends.

the clay particles to reside both at the interphase between the PS and the elastomeric phase, and inside the elastomeric phase may be the hydrophilic characteristics of the elastomeric material that attracts filler particles more in comparison to the PS matrix.

SEM Analysis

The fracture surface of the PS based nanocomposites and the binary blends were studied by SEM to observe the effects of elastomer and organoclay addition on the morphology. The average domain size of the dispersed phase was analyzed by using ImageJ software program, and approximately 50–100 domains were analyzed to get an accurate dimension.

PS is a brittle polymer that exhibits straight crack propagation lines. To overcome this drawback, polymer matrix is blended with various types of rubbery materials that are dispersed in the matrix. During impact, the rubber particles dissipate impact energy by transforming it into deformation of themselves, and eventually voids may form. To establish this mechanism, a well defined adhesion of the rubber particles to the matrix is required.[31,32]

Figure 6(a, b) shows the SEM micrographs of PS/SEBS-g-MA and PS/E-BA-GMA binary blends. The droplet shaped domains represent the elastomeric phases, and they are formed by the breaking up of the minor phase during melt mixing. The size and the shape of the dispersed phase are determined by the interfacial tension, rheological properties, volume fractions of the components, melt viscosity, and the complex strain field in the mixer.[33] The average domain sizes of the binary blends calculated are 225 nm for the PS/SEBS-g-MA and 176 nm for the PS/E-BA-GMA blend. As can be seen from Figure 6(b), after stretching, cracks appear around the elastomer domains due to poor interfacial tension between the PS matrix and E-BA-GMA. Although, the rubber phase distributes itself uniformly in the polymer matrix, a stable system could not be achieved. As a result, it can be said that SEBS-g-MA is a better compatibilizer for PS based nanocomposites in comparison to E-BA-GMA. This better compatibility may be attributed to the solubility of polystyrene end block of SEBS in the amorphous polystyrene matrix. The SEM micrograph of the ternary nanocomposites containing E-BA-GMA could not be taken with the same procedure. Because, the samples crumbled into small pieces during the etching process. Thus, their micrographs were obtained from the fracture surfaces without performing etching.

Figure 7 displays the SEM micrographs of the ternary nanocomposites prepared with SEBS-g-MA for three types of organoclays. When compared with the average domain size of the corresponding binary blend, which has an average diameter of 225 nm, the ternary nanocomposites show higher average dispersed domain sizes no matter whether the clay particles are well dispersed or not. If the organoclay particles were dispersed in the PS matrix, the clay platelets would suppress the agglomeration of the elastomeric domains and cause a barrier effect that hinders the recombination of elastomeric domains.[24] However, in the present case the average domain size increases with organoclay addition, because the clay particles reside in the elastomeric phase and at the interphase between PS and elastomeric material. Thus, the domain sizes are enlarged.

DSC Analysis

In the binary PS/organoclay and ternary nanocomposites no significant variations are observed in the glass transition temperature. However, PS/SEBS-g-MA binary blend and PS/SEBS-g-MA/25A ternary nanocomposites showed approximately 4°C reduction in their T_g compared with pure PS. Thus, it can be said that the glass transition temperature decreases slightly as the dispersion state increases. In addition, the solubility of SEBS-g-MA would lower the glass transition of the polystyrene (Table II).

Mechanical Properties

Tensile tests were performed to obtain the response of the nanocomposites to the applied force and the extent to which the specimens elongate before failure. The dispersion level of clay particles and their location, the shape and size of the elastomeric domains in the matrix, and the interaction between the components are all important factors that the mechanical properties depend on.

Tensile properties of the ternary nanocomposites are shown and compared with the tensile properties of PS/elastomer binary blends and PS/organoclay binary composites in Figures 8–10.

Applied Polymer SCIENCE

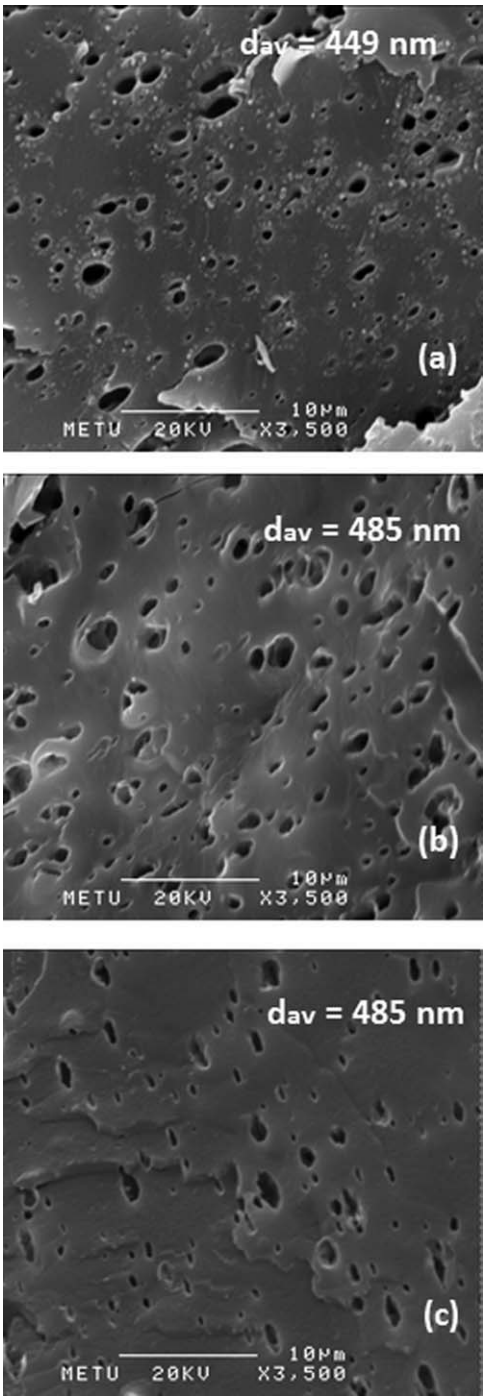

Figure 7. SEM micrographs of PS/SEBS-g-MA/organoclay ternary nanocomposites prepared with: (a) Cloisite® 30B, (b) Cloisite® 15A, and (c) Cloisite® 25A.

Elastomeric materials, SEBS-g-MA and E-BA-GMA, have relatively lower tensile strength and tensile modulus values compared with pure PS. Thus, it is expected that melt mixing of these types of materials with a stiff polymer would result in a dilution effect, and stiffness and/or strength values of PS would decrease. However, with 5 wt % of elastomer loading the reverse of this effect is observed in the binary blends. The reason for the enhancement of the mechanical properties of PS matrix

Table II. Glass Transition Temperature Results

Composition	Concentration		
	Elastomer (wt %)	O-clay (wt %)	T_g (°C)
PS	-	-	108.2
PS + SEBS-g-MA	5	-	104
PS + E-BA-GMA	5	-	108.5
PS + 30B	-	2	109.2
PS + 15A	-	2	108.4
PS + 25A	-	2	108.9
PS + SEBS-g-MA + 30B	5	2	107.8
PS + SEBS-g-MA + 15A	5	2	108.2
PS + SEBS-g-MA + 25A	5	2	105.4
PS + E-BA-GMA + 30B	5	2	107.9
PS + E-BA-GMA + 15A	5	2	109.4
PS + E-BA-GMA + 25A	5	2	110.9

with the addition of 5 wt % elastomeric material can be attributed to the droplet shaped rubbery domains which are formed by the breaking up of the minor phase during melt mixing. This structure prevents early fracture of the PS matrix. This droplet shaped structure defend is present up to 20 wt % elastomer content, then the dispersed morphology turns into a cocontinuous structure leading to reduction in mechanical properties.[34] Although the compatibility between PS and E-BA-GMA is not high compared with the compatibility between PS and SEBS-g-MA, tensile strengths of these two blends are nearly the same. On the contrary, improvement in strain at break and Young's modulus values are higher in the PS/SEBS-g-MA blend.

Subsequent to the addition of organoclay into the binary blends, no significant difference can be observed in the tensile strength values of the ternary nanocomposite containing Cloisite® 30B, whereas Cloisite® 25A containing nanocomposites display slightly enhanced strength values . Especially, the PS/SEBS-g-MA/Cloisite® 25A nanocomposite shows the highest improvement owing to fine dispersion of silicate layers which creates large contact area and thus contributes to the reinforcement effect. The tensile strengths of all the ternary

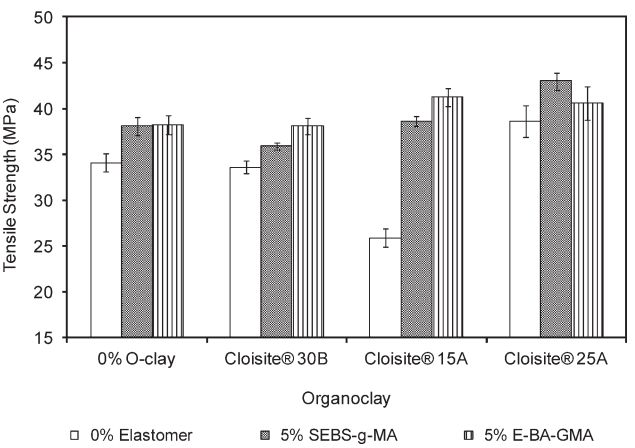

Figure 8. Tensile strength results.

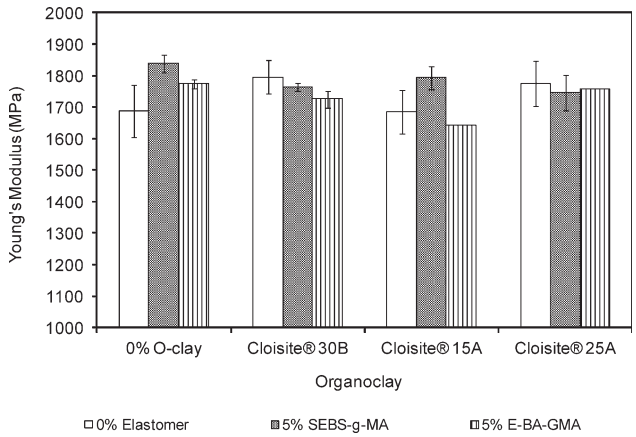

Figure 9. Young's modulus results.

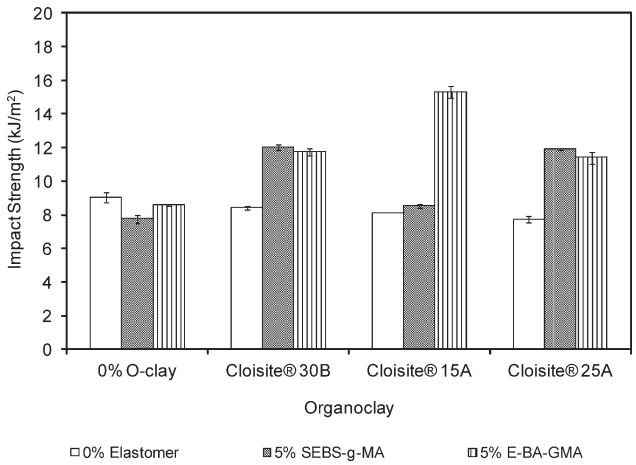

Figure 11. Impact strength results.

nanocomposites are greater than that of pure PS. In PS/organoclay binary nanocomposites a reduction in strength is obvious except for the one prepared with Cloisite® 25A. Thus, it is concluded that the effect of elastomeric material on the improvement of tensile strength is more dominant than the effect of organoclay.

When the stiffnesses of the binary and ternary nanocomposites are considered, no significant variation can be observed compared with the stiffness of the binary blends. However, as in the case of tensile strength results, most of the ternary nanocomposites show a slight enhancement in the Young's modulus values.

Well dispersed organoclay particles stiffen the polymer matrix, while, a drastic reduction in the elongation at break value is commonly observed, because silicate particles cannot be strained by external stresses.[35] Thus, no improvement can be observed in the strain at break values of PS/organoclay binary composites. However, uniformly distributed elastomeric domains and the presence of partially exfoliated and partially intercalated clay layers in these domains increased the strain at break value of the PS/SEBS-g-MA/Cloisite® 25A nanocomposite compared with the strain at break of pure PS. The location of organoclay platelets is important for the elongation of nanocomposite materials because the matrix mobility can be decreased by the

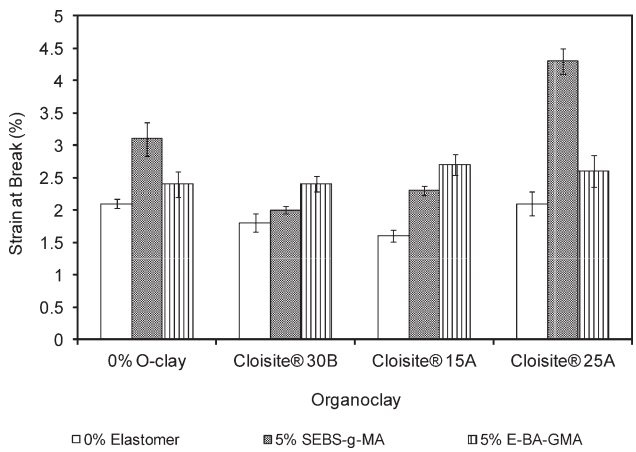

Figure 10. Strain at break results.

presence of delaminated organoclay, if it is dispersed in the polymer matrix.[24] However, in the present case, the exfoliated layers that reside in the elastomeric domains lead to higher elongation at break values.

The effectiveness of rubber phase in the improvement of toughness is directly related to the size of the dispersed elastomeric domains in the polymer matrix. As the domain size increases up to a certain value, the impact strength increases owing to the decrease in the stress concentration effect of the domains. If there is high adhesion between the domains, ultrafine domains of elastomers are formed and these domains lead to low impact strength values, because crack propagation lines progress without touching the elastomeric domains. In addition, the domain size should not be too large, because with large domains large cavities are formed on deformation that cannot stop the crack propagation and lead to early failure. Figure 11 shows the impact strength results of the nanocomposites and binary blends. As expected, rubber modified PS exhibits higher toughness than pure PS, because the elastomeric domains prevent crazes from developing into cracks if there is well defined adhesion of the rubber particles to the matrix.[31,32] However, with 5 wt % of SEBS-g-MA and E-BA-GMA loading, no improvement can be observed in the impact strength. Instead, a slight reduction is obtained. This can be attributed to the ultrafine domain structure at low elastomer contents. When, binary nanocomposites are considered, impact strength values are similar to that of pure PS. However, ternary nanocomposites show higher impact strength values compared with both pure PS and PS/elastomer binary blends owing to enlarged elastomeric domains with organoclay addition. With different organoclay types, no significant difference can be observed in the toughness of the ternary nanocomposites.

CONCLUSIONS

Organoclay Cloisite® 30B showed the worst degree of delamination owing to the hydroxyl groups on its modifier and the incompatibility between the clay surface and middle blocks of the elastomers. A better dispersion is expected for the

nanocomposites containing Cloisite® 15A owing to its lower polar characteristics compared with Cloisite® 25A. However, it is hard for polymer chains to exfoliate the clay layers due to the obstruction created by the two long aliphatic tails of Cloisite® 15A. Thus, the best dispersion was achieved in ternary nanocomposites prepared with Cloisite® 25A, by the introduction of SEBS-g-MA as compatibilizer into the system, because its addition increased the viscosity and thus the shear stress exerted. Although, fully exfoliated layers were observed from the XRD analysis, TEM image of this nanocomposite revealed that partially intercalated and partially exfoliated structures were present. Owing to the hydrophilic characteristics of the elastomeric materials, the clay particles reside inside the dispersed phase and at the interphase between PS and rubber. Thus, in the presence of clay particles, the average elastomer domain size increased.

The soluble part of SEBS-g-MA with PS provided high compatibility between the two phases and made SEBS-g-MA a better impact modifier in PS based nanocomposites compared with E-BA-GMA.

Ternary nanocomposites prepared with Cloisite® 30B showed no improvement in tensile strength compared with binary blends, whereas, enhancement was observed in the strength of the PS/SEBS-g-MA/Cloisite® 25A nanocomposite. The tensile strength and Young's modulus results indicated that elastomeric materials affected these properties more than the organoclays did. The strain at break value of the PS/SEBS-g-MA/Cloisite® 25A nanocomposite was twice that of pure PS owing to the delaminated clay particles that reside inside the elastomeric domains. The impact strength of the ternary nanocomposites was higher than the impact strength of polystyrene and PS/elastomer blends, because the average elastomer domain size increased when organoclay was added, and this minimized the propagation rate of cracks.

ACKNOWLEDGMENTS

This work was supported by The Scientific and Technological Research Council of Turkey (TUBITAK) under contract number 106T425.

REFERENCES

1. Lebaron, P. C.; Wang, Z.; Pinnavaia, T. J. *Appl. Clay Sci.* **1999,** *15*, 11.
2. Alexandre, M.; Dubois, P. *Mater. Sci. Eng.* **2000,** *28*, 1.
3. Mark, J. E. *Polym. Eng. Sci.* **1996,** *36*, 2905.
4. Werne, T.; Patten, T. E. *J. Am. Chem. Soc.* **1999,** *121*, 7409.
5. Herron, N.; Thorn, D. L. *Adv. Mater.* **1998,** *10*, 1173.
6. Giannelis, E. P. *Proceedings of 57th SPE Annual Technical Conference (ANTEC),* **1999;** *Vol. 155*, p 3966.
7. Tjong, S. C. *Mater. Sci. Eng.* **2006,** *53*, 73.
8. Pinnavaia, T. J.; Beall, G. W. Polymer-Clay Nanocomposites; Wiley: England, **2000.**
9. Kroschwitz, J. I. Encyclopedia of Polymer Science and Technology, 3rd ed.; Wiley: Hoboken, NJ, **2003.**
10. Krishnamoorti, R.; Vaia, R. *A; Giannelis, E. P. Chem. Mater.* **1996,** *8*, 1728.
11. Dennis, H. R.; Hunter, D. L.; Chang, D.; Kim, S.; White, J. L.; Cho, J. W.; Paul, D. R. *Polymer* **2001,** *42*, 9513.
12. Bruzaud, S.; Grohens, Y.; Ilinca, S.; Carpentier, J. F. *Macromol. Mater. Eng.* **2005,** *290*, 1106.
13. Chen, B; Evans, J. R.; Greenwell, H. C.; Boulet, P.; Coveney, P. V.; Bowdenf, A. A.; Whiting, A. *Chem. Soc. Rev.* **2008,** *37*, 568.
14. Vaia, R. A.; Jandt, K. D.; Kramer, E. J.; Giannelis, E. P. *Macromolecules* **1995,** *28*, 8080.
15. Vaia, R. A.; Klaus, D.; Kramer, E. J.; Giannelis, E. P. *Chem. Mater.* **1996,** *8*, 2628.
16. Vaia, R. A.; Giannelis, E. P. *Macromolecules* **1997,** *30*, 7990.
17. Vaia, R. A.; Giannelis, E. P. *Macromolecules* **1997,** *30*, 8000.
18. Park, C. I.; Choi, W. M.; Kim, M. H.; Park, O. O. *J. Polym. Sci. Part B: Polym. Phys.* **2004,** *42*, 1685.
19. Sepehr, M.; Utracki, L. A.; Zheng, X.; Wilkie, C. A. *Polymer* **2005,** *46*, 11557.
20. Tanoue, S.; Hasook, A.; Itoh, A.; Yanou, M.; Lemoto, Y.; Unryu, T. J. *Appl. Polym. Sci.* **2006,** *101*, 1165.
21. Park, C. I.; Park, O. O.; Lim, J. G.; Kim, H. J. *Polymer* **2001,** *42*, 7465.
22. Brindley, G. W.; Brown, G. Crystal Structures of Clay Minerals and Their X-Ray Identification; Mineralogical Society: London, **1980.**
23. Huang, X.; Lewis, S.; Brittain, W. J.; Vaia, R. A. *Macromolecules* **2000,** *33*, 2000.
24. Mert, M.; Yilmazer, U. J. *Appl. Polym. Sci.* **2008,** *108*, 3890.
25. Paul, D. R.; Zheng, Q. H.; Yu, A. B.; Lu, G. Q. *J. Colloid Interface Sci.* **2005,** *292*, 42.
26. Isik, I.; Yilmazer, U.; Bayram, G. *Polym. Compos.* **2007,** *29*, 133.
27. Finnigan, B.; Martin, D.; Halley, P.; Truss, R.; Campell, K. J. *Appl. Polym. Sci.* **2005,** *97*, 300.
28. Fornes, T. D.; Yoon, P. J.; Paul, D. R. *Polymer* **2003,** *44*, 7545.
29. Lee, K. M.; Han, C. D. *Macromolecules* **2003,** *36*, 7165.
30. Chow, W. S.; Teoh, J. K.; Lim, L. Y. *Polym. Plast. Technol. Eng.* **2008,** *47*, 1040.
31. Bucknall, C. B. Toughned Plastics; Applied Science Publishers: London, **1977.**
32. Kramer, E. J.; Krauch, H. H. Crazing in Polymers; Springer: Berlin, **1983.**
33. Joseph, S.; Rutkowska, M.; Jastrzêbska, M.; Janik, H.; Haponiuk, J. T.; Thomas, S. J. *Appl. Polym. Sci.* **2003,** *89*, 1007.
34. Yeniova, C.; Yilmazer U. *Polym. Compos.* **2010,** *31*, 1853.
35. Joseph, S.; Rutkowska, M.; Jastrzêbska, M.; Janik, H.; Haponiuk, J. T.; Thomas, S. J. *Appl. Polym. Sci.* **2003,** *89*, 1007.